Giant Amplification of Noise in Fluctuation-Induced Pattern Formation

Tommaso Biancalani,* Farshid Jafarpour, and Nigel Goldenfeld
Department of Physics, University of Illinois at Urbana-Champaign, Loomis Laboratory of Physics, 1110 West Green Street, Urbana, Illinois, 61801-3080, USA
and Carl R. Woese Institute for Genomic Biology, University of Illinois at Urbana-Champaign, 1206 West Gregory Drive, Urbana, Illinois 61801, USA
(Received 11 June 2016; published 3 January 2017)

The amplitude of fluctuation-induced patterns might be expected to be proportional to the strength of the driving noise, suggesting that such patterns would be difficult to observe in nature. Here, we show that a large class of spatially extended dynamical systems driven by intrinsic noise can exhibit giant amplification, yielding patterns whose amplitude is comparable to that of deterministic Turing instabilities. The giant amplification results from the interplay between noise and nonorthogonal eigenvectors of the linear stability matrix, yielding transients that grow with time, and which, when driven by the ever-present intrinsic noise, lead to persistent large amplitude patterns. This mechanism shows that fluctuation-induced Turing patterns are observable, and are not strongly limited by the amplitude of demographic stochasticity nor by the value of the diffusion coefficients.

DOI: 10.1103/PhysRevLett.118.018101

Since the seminal paper of Turing [1], it has been recognized that pattern forming dynamical instabilities could potentially underlie various examples of biological pattern formation and development [2,3]. The Turing mechanism has two major assumptions: first, that two chemical species behave as an activator-inhibitor system (but see a recent extension [4]), and second, that the spatial diffusion constant of the inhibitor is greater than that of the activator, typically by 2 orders of magnitude or more [5,6]. However, this second condition is not generally present in experimental observations [7,8]. The widely held conclusion is that biological patterns reflect gene expression and the interplay of developmental processes, so that the Turing mechanism itself is not generally operative [9].

This conclusion relies upon a third assumption of Turing patterns: that they are deterministic. However, many biological systems exhibit strong fluctuations due to demographic stochasticity (or small number fluctuations), arising from, e.g., finite population size (ecology) or copy number (gene expression) [10,11], and these fluctuations could potentially couple to the underlying pattern-forming instabilities. Detailed analysis shows that the length scale of fluctuation-induced patterns is set by the same condition as in the deterministic Turing analysis, but remarkably the pattern exists over a wide range of parameter values, even where the diffusion constants of activator and inhibitor are of similar magnitudes [5,12–17]. These fluctuation-induced or stochastic patterns arise physically because, even though the uniform unpatterned state is linearly stable, the demographic fluctuations are constantly pushing the system slightly away from its stable fixed point; if the resulting small amplitude dynamics is dominated by an eigenvalue with a nonzero wavelength, then a spatial pattern can arise.

Unfortunately, this mechanism suggests that the amplitude of fluctuation-induced patterns would be set by $\Omega^{-1/2}$, where Ω indicates the total number of molecules within a correlation volume of the system, i.e., the spatial patch within which the system can be considered to be well mixed [12,13]. Thus, in situations where $\Omega \gg 1$, fluctuation-induced patterns would have a very small amplitude compared to deterministic Turing patterns, and so might not be observable nor relevant to biological and ecological pattern formation [18].

The purpose of this Letter is to show that fluctuation-induced Turing patterns can in fact be readily observed, even when the noise is very small and the ratio of diffusion constants is close to one. The new ingredient to the theory uncovered here is the presence of giant amplification, due to an interplay between demographic stochasticity and nonorthogonality of the eigenvectors of the linear stability

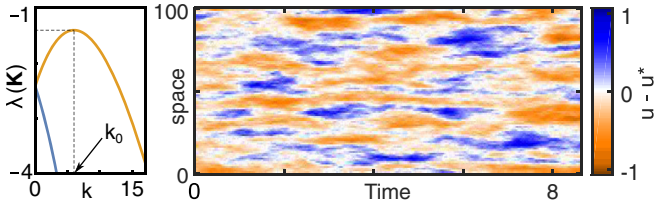

FIG. 1. Turing-like pattern with large amplitude and comparable diffusivities. Right: Stochastic simulations [20] of a two-species model Eq. (8) with diffusivities $\delta_U = 3.9$, $\delta_V = 3.4\delta_U$ and system size $\Omega = 10^4$. Patterns are noise induced as they arise from a stable homogeneous state u^*; i.e., the eigenvalues λ plotted against the wavelength k are negative (left-hand panel). However, despite the small noise, these patterns exhibit an amplitude of order 1 (right bar). Other parameters are $a = 3$, $b = 5.8$, $c = e = 1$.

operator about the uniform stable steady state. In the related problem of noise-induced population cycles in predator-prey systems, amplification arises due to a resonance of the noise with a complex eigenvalue arising from the linearized stability about the time-independent state [19]. In fluctuation-induced stationary Turing patterns, this mechanism cannot be relevant, because the eigenvalues are real, not complex, and so there can be no resonant amplification [12,13]. Our analytical theory shows that giant amplification occurs in a wide class of fluctuation-induced pattern-forming systems, and is a source of amplification distinct from the population-size-dependent resonance that was already identified to arise in spatially uniform quasicycles [19].

An example of our key result described below is shown in Fig. 1: stochastic simulations of the generic pattern-forming model of Ridolfi *et al.* [21], performed on a linear chain of 10^2 spatial cells, each cell with a system size of $\Omega = 10^4$. Patterns are noise induced as they arise from a stable homogeneous state (left-hand panel), but despite the factor $\Omega^{-1/2} = 10^{-2}$, the resulting amplitude is of order unity.

This giant amplification is due to the counterintuitive fact that the dynamics following a small displacement from a stable fixed point need not relax back to the fixed point monotonically: there can be an initial transient amplification if the linear stability matrix is non-normal: that is, it does not admit an orthogonal set of eigenvectors (Fig. 2). Non-normality has been thoroughly investigated at a deterministic level in fluid dynamics [22–24], and in ecology [25,26], and is a common feature of pattern-forming systems [21,27,28]. The specific contribution of the present Letter is to systematically analyze the behavior of non-normal systems in the presence of intrinsic noise. Numerical results of shear flow turbulence [29] indicate that non-normality can increase the variance of stochastic forcing in well-mixed systems, yet an analytical treatment is still missing. Our work treats the role of non-normality in fluctuation-induced spatial patterns, and shows that its widespread occurrence suggests a new way in which fluctuation-induced Turing patterns are amplified and thus

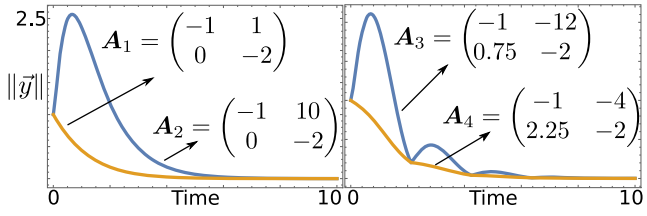

FIG. 2. Stable linear systems can amplify perturbations [25]. Dynamics of the Euclidean norm $\|\vec{y}\|$ obtained by solving $\dot{\vec{y}} = \boldsymbol{A}_i\vec{y}$. Reactive systems exhibit transient amplification before relaxing to fixed point (blue lines), in contrast with conventional response of stable systems (yellow lines). Matrices $\boldsymbol{A}_1$ and $\boldsymbol{A}_2$ ($\boldsymbol{A}_3$ and $\boldsymbol{A}_4$) have the same real (complex conjugate) eigenvalues.

potentially play a wider role in biological and ecological pattern formation than previously recognized.

Non-normality in stochastic dynamics.—We begin by quantifying the degree of amplification in a well-mixed stochastic system. Consider the linear stochastic differential equation for an m-component state vector $\vec{y}$:

$$\dot{\vec{y}} = \boldsymbol{A}\vec{y} + \sigma\vec{\eta}(t), \tag{1}$$

where the components of $\vec{\eta}$, are normalized Gaussian white noises and the model-dependent matrix $\boldsymbol{A}$ has negative real eigenvalues, λ_i $(i = 1, \ldots, m)$. Therefore, the fixed point $\vec{y}_0 = 0$ is stable. The coefficient σ represents the strength of the fluctuations and scales with the system size $\Omega^{-1/2}$ in the case of demographic noise. Equation (1) is the prototypical linearization of stochastic dynamics near a stable fixed point, and we analyze the mean squared displacement from the fixed point $\langle\|\vec{y}\|^2\rangle$, where $\|\vec{y}\| = \sqrt{\vec{y}^T\vec{y}}$, is the Euclidean norm.

Since all the eigenvalues of $\boldsymbol{A}$ are negative, under the deterministic part of Eq. (1), all the components of $\vec{y}$ decay exponentially to zero along the eigenvectors of $\boldsymbol{A}$, with decay time scales $\tau_i = \lambda_i^{-1}$. In contrast, the noise term provides stochastic agitation with a strength proportional to σ. One might intuitively expect that an upper bound for $\langle\|\vec{y}\|^2\rangle$ could be found by replacing all the eigenvalues by the eigenvalues corresponding to the slowest decaying mode, $\lambda = \max\{\lambda_i\}$. Therefore, the norm of $\vec{y}_u$ with the dynamics $\dot{\vec{y}}_u = \lambda\vec{y}_u + \sigma\vec{\eta}(t)$ should provide an upper bound for $\|\vec{y}\|$. The mean squared norm of $\vec{y}_u$ is readily given by $\langle\|\vec{y}_u\|^2\rangle = -m\lambda^{-1}\sigma^2/2$.

However, this upper bound is only valid when the matrix $\boldsymbol{A}$ is normal; i.e., it has an orthogonal set of eigenvectors [29]. This can be understood by analyzing the behavior of Eq. (1) in the deterministic limit ($\sigma = 0$). Although the asymptotic decay rate of $\|\vec{y}\|$ is set by the eigenvalues of $\boldsymbol{A}$, the instantaneous response is given by the eigenvalues of $\boldsymbol{H} = (\boldsymbol{A} + \boldsymbol{A}^T)/2$, the Hermitian part of $\boldsymbol{A}$ [25]. If $\boldsymbol{A}$ is non-normal, then the short-time dynamics of $\|\vec{y}\|$ cannot be predicted by the eigenvalues of $\boldsymbol{A}$. Remarkably, $\boldsymbol{H}$ can admit positive eigenvalues even though $\boldsymbol{A}$ possesses all negative eigenvalues, in which case $\|\vec{y}\|$ can experience a transient growth, for suitable initial conditions, before it starts decaying (Fig. 2). This mechanism, sometimes termed as reactivity [25], occurs because the transformation that takes $\vec{y}$ to the eigenbasis of $\boldsymbol{A}$ is not unitary if the eigenvectors of $\boldsymbol{A}$ are not orthogonal, and thus does not preserve the norm of $\vec{y}$. Clearly, if the stable matrix amplifies perturbations, the previous bound cannot hold.

In the presence of noise, the transient amplification in the deterministic part of Eq. (1) has a lasting effect on the steady-state amplitude of the stochastic dynamics. We demonstrate this by computing the mean squared norm for Eq. (1) [see the detailed derivation in the Supplemental Material (SM) [30]]:

$$\langle \|\vec{y}\|^2 \rangle = -\frac{\sigma^2}{2}\mathcal{H}(\boldsymbol{A})\mathrm{tr}(\boldsymbol{A}^{-1}), \tag{2}$$

where tr stands for the trace function and we define $\mathcal{H}$ as the non-normality index. The term $\mathrm{tr}(\boldsymbol{A}^{-1})$ is the conventional term that accounts for the matrix stability: the more stable the matrix, the smaller the mean squared norm of $\vec{y}$ due to stochastic forcing. In contrast, the non-normality index is a real number always, $\mathcal{H} \geq 1$, and is equal to one if and only if the matrix $\boldsymbol{A}$ admits a basis of orthogonal eigenvectors. This is the term that accounts for amplification due to the non-normality of matrix $\boldsymbol{A}$, and indeed, the further $\boldsymbol{A}$ is from normal, the larger is the index $\mathcal{H}$. We can obtain intuition about the non-normality index in the case of a two-dimensional matrix $\boldsymbol{A}$, where the non-normality index $\mathcal{H}$ simplifies to the following simple expression, where $\cot\theta$ is the cotangent of the angle between the two eigenvectors (see SM for derivation and general formulas [30]):

$$\mathcal{H} = 1 + \cot^2(\theta)\left(\frac{\lambda_1 - \lambda_2}{\lambda_1 + \lambda_2}\right)^2. \tag{3}$$

This expression gives us quantitative understanding about how transient amplification occurs (Fig. 3). Two ingredients are necessary: nonorthogonal eigenvectors and a separation of time scales given by eigenvalues of different magnitudes. If the system is not subject to noise, suitable initial conditions are also required (e.g., the blue vector in Fig. 3). Because of the separation of time scales, the component of $\vec{y}$ along the eigenvector associated with the faster eigenvalue decays quickly, whereas in the slow direction the dynamics is approximately constant. However, because of nonorthogonality, the norm of $\vec{y}$ instantaneously increases as $\vec{y}$ moves along the fast eigenvector, until the slow manifold starts attracting the trajectory back to the fixed point.

Non-normality in spatially extended pattern formation.—We now analyze spatially extended, diffusively coupled pattern-forming systems driven by noise. Specifically, we consider the generic equation

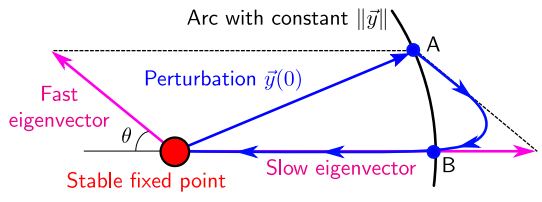

FIG. 3. Transient amplification is caused by nonorthogonal eigenvectors and a separation of time scales. The stable fixed point is subject to the perturbation $\vec{y}(0)$. Because of the separation of time scales, the deterministic trajectory (blue arrowed line) is initially parallel to the fast eigenvector before relaxing to the slow manifold. From A to B, the trajectory has magnitude greater than $||\vec{y}_0||$.

$$\frac{\partial \vec{q}}{\partial t} = \vec{f}(\vec{q}) + \boldsymbol{D}\nabla^2\vec{q} + \sigma\vec{\xi}(\vec{x}, t), \tag{4}$$

where $\vec{x}$ is a space variable, the vector $\vec{q} = (q_1, q_2)$, the diffusion matrix $\boldsymbol{D} = \mathrm{diag}(D_1, D_2)$, and ξ_i's, the components of $\vec{\xi}(\vec{x}, t)$, are normalized δ-correlated Gaussian white noises. Also, we assume that $\vec{f}(\vec{q})$ has a stable fixed point $\vec{q}^*$, and all of the eigenvalues of the linear stability or Jacobian matrix $\boldsymbol{J} = \nabla_{\vec{q}} f(\vec{q})|_{\vec{q}^*}$ have negative real part.

We first show that in the presence of noise, system Eq. (4) exhibits patterns in a parameter regime where the fixed point $\vec{q}^*$ is stable. The stability of $\vec{q}^*$ can be inspected by defining the deviation $\vec{p} = \vec{q} - \vec{q}^*$ and linearizing near $\vec{q}^*$, yielding

$$\frac{\partial \vec{p}}{\partial t} = \boldsymbol{J}\vec{p} + \boldsymbol{D}\nabla^2\vec{p} + \sigma\vec{\xi}(\vec{x}, t). \tag{5}$$

The spatial degrees of freedom can be diagonalized by a Fourier transform ($\vec{x} \mapsto \vec{k}$), resulting in

$$\frac{d\vec{p}_{\vec{k}}}{dt} = \boldsymbol{K}\vec{p}_{\vec{k}} + \sigma\vec{\xi}(\vec{k}, t), \qquad \boldsymbol{K} = \boldsymbol{J} - k^2\boldsymbol{D}. \tag{6}$$

Equation (6) is a complex version of Eq. (1).

We start by reviewing the stability of the deterministic part of Eq. (5). If $D_1 = D_2$, matrix $\boldsymbol{D}$ is a multiple of the identity, and the eigenvalues of $\boldsymbol{K}$ will be the eigenvalues of $\boldsymbol{J}$ shifted by $-k^2D$ for each $\vec{k}$, resulting in a more stable operator. However, in the case that the diffusion rates are sufficiently different, the largest eigenvalue of $\boldsymbol{K}$ can have a nonmonotonic behavior as a function of k^2, and in some cases have positive eigenvalues for a small range of $\vec{k}$ peaked around some nonzero value $\vec{k}_0$. In this case, the modes near $\vec{k}_0$ will grow, leading to the formation of deterministic Turing patterns [1]. Therefore, the formation of deterministic Turing patterns is dependent on a large separation of the diffusion constants [6–8].

In contrast, consider an intermediate scenario with diffusion constants different enough so that they can cause a nonmonotonic behavior for the largest eigenvalue of $\boldsymbol{K}$ as a function of k^2 peaked around some value $\vec{k}_0$, but not enough for the largest eigenvalue to be positive at $\vec{k}_0$ (left-hand panel of Fig. 1). In this case, all the $\vec{k}$ modes decay quickly to zero, but the modes with $\vec{k} \sim \vec{k}_0$ decay slower than the others, causing a transient pattern. In the presence of the noise term $\vec{\xi}(\vec{k}, t)$ in Eq. (6), while the modes with smaller eigenvalues decay quickly to zero, the slow modes drift away from the fixed point under the influence of the noise. The drift of the $\vec{k}$ modes near $\vec{k}_0$ produces persistent steady-state fluctuation-induced patterns with well-defined length scales [12,13]. While the stochastic Turing patterns

have a less stringent requirement than the deterministic Turing patterns for the ratio of the diffusion constants, their amplitude is limited to the amplitude of the drift under the noise suppressed by the slow deterministic decay. As discussed in the previous section, the mean squared amplitude is of order $\lambda^{-1}\sigma^2$, unless we can show that the system is non-normal.

We now show that in order for a system described by Eq. (4) to produce stochastic patterns, it is necessary for the matrix $\boldsymbol{J}$ in Eq. (5) to be non-normal. The real part of the largest eigenvalue of a normal matrix is equal to that of its Hermitian part. Therefore, we can measure how far from normal the matrix $\boldsymbol{J}$ is by finding a lower bound on the difference between the largest eigenvalue of $\boldsymbol{H} = (\boldsymbol{J} + \boldsymbol{J}^T)/2$ and that of matrix $\boldsymbol{J}$ (the proof of this inequality is given in SM [30]):

$$\lambda_1(\boldsymbol{H}) - \mathrm{Re}(\lambda_1(\boldsymbol{J})) \geq \delta + k_0^2 D_{\min}, \tag{7}$$

where $\delta = \mathrm{Re}(\lambda_1[\boldsymbol{K}(\vec{k}_0)]) - \mathrm{Re}(\lambda_1(\boldsymbol{J})) > 0$, $\vec{k}_0$ is the wave vectors at which the real part of the largest eigenvalue peaks, and $D_{\min}$ is the smallest of the diffusion constants.

Since the non-normality of $\boldsymbol{J}$ should be independent of the diffusion constants, this lower bound can be extended to the supremum of the right-hand side of the inequality Eq. (7) over all the matrices $\boldsymbol{D}$ that produce spatial patterns and their corresponding $\vec{k}_0$. In particular, if a system admits deterministic Turing patterns for some set of diffusion constants, this inequality implies that the matrix $\boldsymbol{J}$ would be reactive [i.e., $\lambda_1(\boldsymbol{H}) \geq 0$; this special case was previously proven by Neubert *et al.* [27]]. In this case, if experimentally measured values of diffusion constants do not fall within the Turing pattern regime, the system is still reactive and capable of exhibiting amplified stochastic patterns.

Worked-out example.—Finally, we apply our theory to a concrete model that is representative of a large class of systems. The model is given by Eq. (4) with two species U and V with densities $\vec{q} = (u, v)$, and $\vec{f}(u, v) = (u(auv - e), v(b - cu^2 v))$, with $a, b, c, e > 0$ [21]. The corresponding individual-level model is defined by considering the following reactions that occur on a discretized m-dimensional space with L^m lattice sites,

$$\begin{aligned} &2U_i + V_i \xrightarrow{a} 3U_i + V_i, \qquad V_i \xrightarrow{b} 2V_i, \\ &U_i \xrightarrow{e} \emptyset, \qquad 2V_i + 2U_i \xrightarrow{c} V_i + 2U_i, \\ &U_i \xrightarrow{\delta_U} U_j, \qquad V_i \xrightarrow{\delta_V} V_j, \qquad j \in \langle i \rangle, \end{aligned} \tag{8}$$

where U_i and V_i are the species U and V on the site i for $i = 1, \ldots, L^m$ and $\langle i \rangle$ is the set of sites neighboring i. The state of the system is specified by the concentration vectors $\vec{q}_i \equiv (u_i, v_i) \equiv (U_i, V_i)/\Omega$, where Ω is the volume of each site. The diffusion rates δ_u and δ_v are related to the diffusion constants by $(\delta_u, \delta_v) = (D_U, D_V)/\Omega^{2/m}$. The discrete-space version of Eqs. (4)–(6) are derived by expanding in powers of $\Omega^{-1/2}$ the master equation corresponding to scheme Eq. (8) (see SM for the derivations [30]).

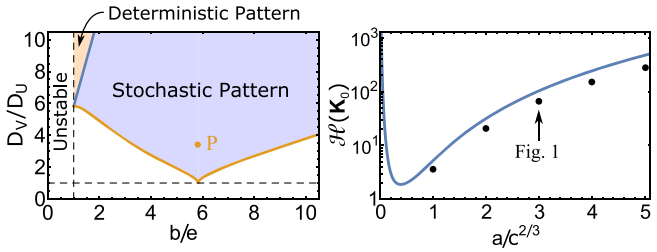

FIG. 4. Stochasticity allows pattern formation for similar diffusivities. Left: Phase diagram of model Eq. (8) showing that the pattern-forming behavior of this model depends only on the ratios b/e and D_V/D_U (see SM for analytical expression for the boundaries [30]). Right: Semi-log plot of non-normality index for the point P as a function of $a/c^{2/3}$. Black markers are amplifications measured in simulations.

The pattern-forming behavior of the model described by Eq. (8) only depends on the ratio of the diffusion constants D_V/D_U and the ratio of the reaction rates of the two linear reactions b/e. The left-hand panel of Fig. 4 shows the regime of parameters in which the system exhibits either stochastic or deterministic Turing patterns [34]. As expected, deterministic patterns emerge only when the ratio D_V/D_U of diffusion constants is very large (above the blue line in Fig. 4, which grows rapidly outside of the figure), while the requirement on this ratio for the stochastic patterns is drastically reduced. In the absence of the non-normality effect, one would expect that only stochastic patterns with parameters very close to the deterministic regime would be observed, since far from this regime, the amplitude of the patterns would be too small to detect.

However, since for all $b/e > 1$ there is a D_V/D_U above which the system exhibits deterministic Turing patterns, $\boldsymbol{J}$ is reactive. Therefore, even when the system is far from the parameter regime of deterministic patterns, the amplitude of the stochastic patterns is far larger than what one would expect from the analysis of the eigenvalues. We can see this by analyzing the amplitude of the patterns at the point P in Fig. 4. This point ($b/e = 5.8$ and $D_V/D_U = 3.4$) is chosen to be very far from the deterministic Turing pattern regime. At this b/e ratio, the ratio of the diffusion constants has to be at least 10 times larger for the system to exhibit deterministic Turing patterns. The amplitude of the patterns as determined by Eq. (2) is dependent on the eigenvalues of $\boldsymbol{K}$ (fixed by the choice of the point P) and the non-normality index $\mathcal{H}(\boldsymbol{K})$, which can be tuned by changing the ratio $a/c^{2/3}$ without changing the point P. The right-hand panel of Fig. 4 shows that the amplification of stochastic patterns for the point P varies over orders of magnitude for a small range of $a/c^{2/3}$.

The right-hand panel of Fig. 1 shows the time series of the amplified stochastic Turing patterns in the concentration of the species U, in a simulation of our model in one dimension (for the point specified in the right-hand panel of Fig. 4). The mean squared amplitude of these spatial patterns is about 0.21, while the upper bound for the amplitude of the pattern in the absence of non-normality is 2.5×10^{-3}. The non-normality index $\mathcal{H}$ (of the slowest Fourier mode $k_0 = 6$) is about 103, justifying the 2 order of magnitude amplification in the amplitude of the stochastic patterns.

This work was supported by the National Aeronautics and Space Administration Astrobiology Institute (NAI) under Cooperative Agreement No. NNA13AA91A issued through the Science Mission Directorate. T. B. acknowledges partial funding from the National Science Foundation under Grant No. PHY-105515.

T. B. and F. J. contributed equally to this work.

*Present address: Physics of Living Systems, Department of Physics, Massachusetts Institute of Technology, Cambridge, MA, USA.

[1] A. M. Turing, Phil. Trans. R. Soc. B **237**, 37 (1952).
[2] A. Koch and H. Meinhardt, Rev. Mod. Phys. **66**, 1481 (1994).
[3] A. D. Economou, A. Ohazama, T. Porntaveetus, P. T. Sharpe, S. Kondo, M. A. Basson, A. Gritli-Linde, M. T. Cobourne, and J. B. Green, Nat. Genet. **44**, 348 (2012).
[4] S. Werner, T. Stückemann, M. Beiran Amigo, J. C. Rink, F. Jülicher, and B. M. Friedrich, Phys. Rev. Lett. **114**, 138101 (2015).
[5] T. Butler and N. Goldenfeld, Phys. Rev. E **84**, 011112 (2011).
[6] J. D. Murray, in *Mathematical Biology. II Spatial Models and Biomedical Applications*, Interdisciplinary Applied Mathematics (Springer-Verlag, New York, 2001), Vol. 18.
[7] V. Castets, E. Dulos, J. Boissonade, and P. De Kepper, Phys. Rev. Lett. **64**, 2953 (1990).
[8] Q. Ouyang and H. L. Swinney, Nature (London) **352**, 610 (1991).
[9] P. K. Maini, T. E. Woolley, R. E. Baker, E. A. Gaffney, and S. S. Lee, Interface Focus **2**, 487 (2012).
[10] M. Mobilia, I. T. Georgiev, and U. C. Täuber, J. Stat. Phys. **128**, 447 (2007).
[11] F. Jafarpour, T. Biancalani, and N. Goldenfeld, Phys. Rev. Lett. **115**, 158101 (2015).
[12] T. Butler and N. Goldenfeld, Phys. Rev. E **80**, 030902 (2009).
[13] T. Biancalani, D. Fanelli, and F. Di Patti, Phys. Rev. E **81**, 046215 (2010).
[14] S. Datta, G. W. Delius, R. Law, and M. J. Plank, J. Math. Biol. **63**, 779 (2011).
[15] L. Ridolfi, P. D'Odorico, and F. Laio, *Noise-Induced Phenomena in the Environmental Sciences* (Cambridge University Press, Cambridge, England, 2011).
[16] J. A. Bonachela, M. A. Muñoz, and S. A. Levin, J. Stat. Phys. **148**, 724 (2012).
[17] T. C. Butler, M. Benayoun, E. Wallace, W. van Drongelen, N. Goldenfeld, and J. Cowan, Proc. Natl. Acad. Sci. U.S.A. **109**, 606 (2012).
[18] A. J. McKane, T. Biancalani, and T. Rogers, Bull. Math. Biol. **76**, 895 (2014).
[19] A. J. McKane and T. J. Newman, Phys. Rev. Lett. **94**, 218102 (2005).
[20] D. T. Gillespie, A. Hellander, and L. R. Petzold, J. Chem. Phys. **138**, 170901 (2013).
[21] L. Ridolfi, C. Camporeale, P. D'Odorico, and F. Laio, Eur. Phys. Lett. **95**, 18003 (2011).
[22] L. N. Trefethen, A. E. Trefethen, S. C. Reddy, and T. A. Driscoll, Science **261**, 578 (1993).
[23] L. N. Trefethen and M. Embree, *Spectra and Pseudospectra: The Behavior of Nonnormal Matrices and Operators* (Princeton University Press, Princeton, NJ, 2005).
[24] A. Roberts, J. Aust. Math. Soc. Series B, Appl. Math. **31**, 48 (1989).
[25] M. G. Neubert and H. Caswell, Ecology **78**, 653 (1997).
[26] S. Tang and S. Allesina, Frontiers in Ecology and Evolution **2**, 21 (2014).
[27] M. G. Neubert, H. Caswell, and J. Murray, Math. Biosci. **175**, 1 (2002).
[28] A. J. Roberts, *Model Emergent Dynamics in Complex Systems* (SIAM, Adelaide, 2014).
[29] B. F. Farrell and P. J. Ioannou, Phys. Rev. Lett. **72**, 1188 (1994).
[30] See Supplemental Material at http://link.aps.org/supplemental/10.1103/PhysRevLett.118.018101, which includes Refs. [31–33], for derivations of Eqs. (2), (3), and (7), general formula for non-normality index, and the complete analysis of the model described in Eq. (8).
[31] C. W. Gardiner, *Handbook of Stochastic Methods for Physics, Chemistry and the Natural Sciences*, 4th ed. (Springer, New York, 2009).
[32] N. G. van Kampen, *Stochastic Processes in Physics and Chemistry*, 3rd ed. (Elsevier Science, Amsterdam, 2007).
[33] M. Adam and M. J. Tsatsomeros, Electron. J. Linear Algebra **15**, 239 (2006).
[34] The region of stochastic patterns is defined as the parameter regime in which the largest eigenvalue of $\boldsymbol{K}$ has a peak at some $\vec{k}_0 \neq 0$ with a value larger than its value at $\vec{k} = 0$.

Supplemental Material for:

Giant amplification of noise in fluctuation-induced pattern formation

Tommaso Biancalani, Farshid Jafarpour and Nigel Goldenfeld

A. Linear response of stochastic non-normal systems

1. The stationary distribution

In the main text, we encounter multiple times the linear stochastic differential equation (SDE) of the form

$$\frac{d\vec{y}}{dt} = \boldsymbol{A}\vec{y} + \vec{\eta}(t), \tag{S1}$$

where $\boldsymbol{A}$ is independent of $\vec{y}$ and $\vec{\eta}$ are Gaussian white noises with zero mean and correlator

$$\langle \vec{\eta}(t)\, \vec{\eta}^{T}(t') \rangle = \boldsymbol{B}\delta(t-t'). \tag{S2}$$

The noise matrix $\boldsymbol{B}$ is symmetric (*i.e* $\boldsymbol{B}^T = \boldsymbol{B}$) and also supposed independent of $\vec{y}$. Equation (S1) is tantamount to the Fokker-Planck equation for the probability density $P(\vec{y}, t)$ [1]:

$$\frac{\partial P(\vec{y},t)}{\partial t} = -\sum_{i,j} A_{ij} \frac{\partial}{\partial y_i}(y_j P) + \frac{1}{2}\sum_{i,j} \frac{\partial^2}{\partial y_i \partial y_j}(B_{ij} P). \tag{S3}$$

As shown in (*e.g.*) [2], the stationary distribution is Gaussian and takes the form

$$P_s(\vec{y}) = \frac{1}{\sqrt{\det(2\pi\boldsymbol{\Xi})}} \exp\left(-\frac{1}{2}\vec{y}^{T}\, \boldsymbol{\Xi}^{-1}\, \vec{y}\right), \tag{S4}$$

where the covariance matrix $\boldsymbol{\Xi}$ is symmetric and given by the Sylvester's equation,

$$\boldsymbol{A}\boldsymbol{\Xi} + \boldsymbol{\Xi}\boldsymbol{A}^T + \boldsymbol{B} = 0. \tag{S5}$$

In two dimensions, this equation can be solved [1] leading to an explicit formula for $\boldsymbol{\Xi}$ ($\mathbb{1}_2$ is the two-dimensional identity matrix):

$$\boldsymbol{\Xi} = \frac{(\boldsymbol{A} - \mathbb{1}_2 \operatorname{tr}\boldsymbol{A})\, \boldsymbol{B}\, (\mathbb{1}_2 \operatorname{tr}\boldsymbol{A} - \boldsymbol{A})^T - \boldsymbol{B} \det \boldsymbol{A}}{2 \operatorname{tr}\boldsymbol{A} \det \boldsymbol{A}}. \tag{S6}$$

2. The stationary mean amplification factor $\langle \|\vec{y}\|^2 \rangle$

We now wish to find an expression for the mean amplification factor, or mean squared norm, $\langle \|\vec{y}\|^2 \rangle$, used in the main text to quantify the linear response of a stochastic non-normal system. The norm of $\vec{y}$ is the Euclidean norm $\|\vec{y}\| = \sqrt{\sum_i |y_i^2|}$. Specifically, we want to compute the integral:

$$\langle \|\vec{y}\|^2 \rangle = \int d\vec{y}\, P_s(\vec{y})\, \|\vec{y}\|^2, \tag{S7}$$

where the distribution $P_s(\vec{y})$ is given by Eq. (S4). Therefore,

$$\langle \|\vec{y}\|^2 \rangle = \frac{1}{\sqrt{\det(2\pi\boldsymbol{\Xi})}} \int d\vec{y} \exp\left(-\frac{1}{2}\vec{y}^{T}\, \boldsymbol{\Xi}^{-1}\, \vec{y}\right) \|\vec{y}\|^2. \tag{S8}$$

To evaluate this integral, we use the identity

$$\int \|\vec{p}\|^2\, e^{-\vec{p}^{\,T}\boldsymbol{M}\vec{p}} d\vec{p} = \frac{1}{2}\mathrm{Tr}\left(\boldsymbol{M}^{-1}\right) \int e^{-\vec{p}^{\,T}\boldsymbol{M}\vec{p}} d\vec{p}, \tag{S9}$$

with $\boldsymbol{M} = 1/2\boldsymbol{\Xi}^{-1}$, which yields the compact expression:

$$\langle \|\vec{y}\|^2 \rangle = \operatorname{Tr} \boldsymbol{\Xi}. \tag{S10}$$

In the following, we assume for convenience that the noise matrix $\boldsymbol{B}$ is a multiple of the identity matrix $\mathbb{1}$ ($\boldsymbol{B} = \sigma^2 \mathbb{1}$), a choice that can be made without losing in generality. In fact, since $\boldsymbol{B}$ is symmetric, it is diagonalized by an orthogonal matrix which one can use to transform the noises; the resulting diagonal matrix can then be mapped to the identity matrix simply by rescaling the variables $\vec{y}$. We now introduce the Hermitianizer of $\boldsymbol{A}$, defined as

$$\boldsymbol{G} = -\frac{1}{2}\, \sigma^2\, \boldsymbol{\Xi}^{-1} \boldsymbol{A}^{-1}. \tag{S11}$$

Even though $\boldsymbol{A}$ is not symmetric, $\boldsymbol{A} \neq \boldsymbol{A}^T$, the product $\boldsymbol{GA} = -2^{-1}\sigma^2 \boldsymbol{\Xi}^{-1}$ is a symmetric matrix. Sylvester equation (S5) written in terms of $\boldsymbol{G}$ simplifies to

$$\frac{1}{2}(\boldsymbol{G}^{-1} + (\boldsymbol{G}^{-1})^T) = \mathbb{1}, \tag{S12}$$

indicating that the Hermitian part of $\boldsymbol{G}^{-1}$ is the identity matrix. Alternatively, the Hermitianizer of $\boldsymbol{A}$ can be defined as the unique matrix satisfying Eq. (S12) whose product with $\boldsymbol{A}$ is Hermitian. We now write the mean squared norm of $\vec{y}$ in terms of $\boldsymbol{A}$ and $\boldsymbol{G}$ by substituting Eq. (S11) in Eq. (S10):

$$\langle \|\vec{y}\|^2 \rangle = -\frac{1}{2}\sigma^2 \operatorname{Tr}\left(\boldsymbol{A}^{-1}\boldsymbol{G}^{-1}\right). \tag{S13}$$

When $\boldsymbol{A}$ is a 2×2 matrix, the trace of the inverse can be written as trace over determinant, yielding

$$\langle \|\vec{y}\|^2 \rangle = -\frac{1}{2}\sigma^2 \frac{\operatorname{Tr}(\boldsymbol{GA})}{\det(\boldsymbol{G})\det(\boldsymbol{A})}. \tag{S14}$$

Taking the trace of Eq. (S11) leads to a simplification of $\operatorname{Tr}(\boldsymbol{GA})$:

$$\operatorname{Tr}(\boldsymbol{GA}) = -\frac{1}{2}\, \sigma^2 \operatorname{Tr}(\boldsymbol{\Xi}^{-1}). \tag{S15}$$

By multiplying the right-hand side of the Sylvester equation (S5) by $\boldsymbol{\Xi}^{-1}$,

$$\boldsymbol{A} + \boldsymbol{\Xi}\boldsymbol{A}^T\boldsymbol{\Xi}^{-1} = -\sigma^2\, \boldsymbol{\Xi}^{-1}, \tag{S16}$$

and taking the trace of the above equation (recalling that $\operatorname{Tr}(\boldsymbol{\Xi}\boldsymbol{A}^T\boldsymbol{\Xi}^{-1}) = \operatorname{Tr}(\boldsymbol{A}^T) = \operatorname{Tr}(\boldsymbol{A})$) we arrive at

$$\sigma^2 \operatorname{Tr}(\boldsymbol{\Xi}^{-1}) = -2 \operatorname{Tr}(\boldsymbol{A}). \tag{S17}$$

From Eq. (S17) and Eq. (S15) it follows that $\operatorname{Tr}(\boldsymbol{GA}) = \operatorname{Tr}(\boldsymbol{A})$, which we can use to simplify Eq. (S13):

$$\langle \|\vec{y}\|^2 \rangle = -\frac{\sigma^2}{2 \det \boldsymbol{G}} \frac{\operatorname{Tr} \boldsymbol{A}}{\det \boldsymbol{A}} = -\frac{1}{2}\, \sigma^2\, \det\left(\boldsymbol{G}^{-1}\right) \operatorname{Tr}\left(\boldsymbol{A}^{-1}\right). \tag{S18}$$

This expression corresponds to Eq. (2) in the main text, with the identification $\mathcal{H}(\boldsymbol{A}) = \det\left(\boldsymbol{G}^{-1}\right)$. Note that when $\boldsymbol{A}$ is Hermitian, the Hermitianizer $\boldsymbol{G}$ is the identity with determinant 1. Then Eq. (S18) without the term $\det(\boldsymbol{G}^{-1})$ is the mean square norm of $\vec{y}$ for a normal matrix, and the term $\det(\boldsymbol{G}^{-1})$ can be interpreted as the amplification factor due to nonnormality.

3. Explicit formula for the non-normality index for a two-dimensional matrix

For a 2×2 matrix $\boldsymbol{A}$ given by its elements

$$\boldsymbol{A} = \begin{pmatrix} a_{11} & a_{12} \\ a_{21} & a_{22} \end{pmatrix}, \tag{S19}$$

we can solve for $\boldsymbol{\Xi}$ from Eq. (S6) and substitute in Eq. (S11) to find the matrix $\boldsymbol{G}$ in terms of matrix elements of $\boldsymbol{A}$. We find that

$$\boldsymbol{G} = \begin{pmatrix} \frac{(a_{11}+a_{22})^2}{(a_{12}-a_{21})^2+(a_{11}+a_{22})^2} & -\frac{(a_{12}-a_{21})(a_{11}+a_{22})}{(a_{12}-a_{21})^2+(a_{11}+a_{22})^2} \\ \frac{(a_{12}-a_{21})(a_{11}+a_{22})}{(a_{12}-a_{21})^2+(a_{11}+a_{22})^2} & \frac{(a_{11}+a_{22})^2}{(a_{12}-a_{21})^2+(a_{11}+a_{22})^2} \end{pmatrix}. \tag{S20}$$

The non-normality index $\mathcal{H}$ is given by the inverse of the determinant of $\boldsymbol{G}$:

$$\mathcal{H}(\boldsymbol{A}) = \det\left(\boldsymbol{G}^{-1}\right) = 1 + \frac{(a_{12}-a_{21})^2}{(a_{11}+a_{22})^2}. \tag{S21}$$

If the eigenvalues of $\boldsymbol{A}$ are real, we can rewrite this expression in terms of the eigenvalues, and the angle between the eigenvectors of $\boldsymbol{A}$. Let $\Delta > 0$ be the discriminant of the characteristic polynomial of $\boldsymbol{A}$:

$$\Delta = (a_{11}-a_{22})^2 + 4\,a_{12}\,a_{21}. \tag{S22}$$

If λ_1 and λ_2 are the two eigenvalues of $\boldsymbol{A}$, and $\vec{v}_1$ and $\vec{v}_2$ are the two eigenvectors, we have

$$\begin{aligned} &(\lambda_1+\lambda_2)^2 = (a_{11}+a_{22})^2, \qquad (\lambda_1-\lambda_2)^2 = \Delta, \\ &\cos^2(\theta) = \left(\frac{\vec{v}_1\cdot\vec{v}_2}{\|\vec{v}_1\|\,\|\vec{v}_2\|}\right)^2, \qquad \cot^2(\theta) = \frac{\cos^2(\theta)}{1-\cos^2(\theta)} = \frac{(a_{11}-a_{22})^2}{\Delta}. \end{aligned} \tag{S23}$$

Now it is clear that

$$\mathcal{H}(\boldsymbol{A}) = 1 + \cot^2(\theta)\left(\frac{\lambda_1-\lambda_2}{\lambda_1+\lambda_2}\right)^2. \tag{S24}$$

4. *Linear stochastic differential equations with complex variables*

We would like to apply the results of Sections A 1 and A 2 to the Fourier mode of spatially extended systems. However, Fourier variables are complex-valued, and we need to derive these results for a complex version of Eq. (S1). Consider a similar set of SDEs of the the form

$$\frac{d\vec{y}}{dt} = \boldsymbol{A}\vec{y} + \vec{\eta}(t), \tag{S25}$$

where now $\vec{y}$ and $\vec{\eta}$ are vectors with complex variables, and $\vec{\eta}$ is a Gaussian white noise with zero mean and correlator

$$\begin{aligned} &\langle \vec{\eta}(t)\,\vec{\eta}^{\,\dagger}(t')\rangle = \boldsymbol{B}\delta(t-t'), \\ &\langle \vec{\eta}(t)\,\vec{\eta}^{\,T}(t')\rangle = 0. \end{aligned} \tag{S26}$$

where the † symbol represents the transpose conjugate. The analysis in the previous section can be generalized by evaluating the expected value of $\vec{y}(t)\vec{y}^{\,\dagger}(\tau)$ and $\vec{y}(t)\vec{y}^{\,T}(\tau)$ at steady state for $t=\tau$ to obtain the following relationships for the *covariance* and *relation* matrices

$$\begin{aligned} &\boldsymbol{A}\left\langle \vec{y}\vec{y}^{\,\dagger}\right\rangle + \left\langle \vec{y}\vec{y}^{\,\dagger}\right\rangle \boldsymbol{A}^\dagger + \boldsymbol{B} = 0 \\ &\boldsymbol{A}\left\langle \vec{y}\vec{y}^{\,T}\right\rangle + \left\langle \vec{y}\vec{y}^{\,T}\right\rangle \boldsymbol{A}^T = 0 \end{aligned} \tag{S27}$$

The first equation is the analogue of equation of Sylvester Eq. (S5) for the Hermitian covariance matrix $\boldsymbol{\Xi} = \left\langle \vec{y}\vec{y}^{\,\dagger}\right\rangle$, while the second equation implies that the symmetric relation matrix $\boldsymbol{C} = \left\langle \vec{y}\vec{y}^{\,T}\right\rangle$ is equal to zero. Therefore, at steady state, $\vec{y}$ obeys a circularly symmetric complex Gaussian distribution of the form

$$P_s(\vec{y}) = \frac{1}{\det(2\pi\boldsymbol{\Xi})}\exp\left(-\frac{1}{2}\vec{y}^{\,\dagger}\,\boldsymbol{\Xi}^{-1}\,\vec{y}\right). \tag{S28}$$

Notice the different normalization factor compared to Eq (S4), as it is normalized over $\mathbb{C}^D$ instead of $\mathbb{R}^D$.

To compute the mean squared norm of $\vec{y}$, we can follow similar analysis to that of section A 2. Here, we highlight the differences. The mean squared norm is defined as

$$\langle \|\vec{y}\|^2 \rangle = \int_{\mathbb{C}^D} d\vec{y}\, P_s(\vec{y})\, \|\vec{y}\|^2 , \tag{S29}$$

with the norm $\|\vec{y}\| = \sqrt{\vec{y}^\dagger \vec{y}}$. The complex version of Eq. (S9) can be evaluated by diagonalizing the matrix $\boldsymbol{M}$ and write the integral on a $2D$-dimensional real space. The result is given by

$$\int_{\mathbb{C}^D} \|\vec{p}\|^2\, e^{-\vec{p}^\dagger \boldsymbol{M} \vec{p}} d\vec{p} = \mathrm{Tr}\left(\boldsymbol{M}^{-1}\right) \int_{\mathbb{C}^D} e^{-\vec{p}^\dagger \boldsymbol{M} \vec{p}} d\vec{p}, \tag{S30}$$

where the factor $1/2$ is canceled by the fact that each eigenvalue of $\boldsymbol{M}^{-1}$ should be counted twice in the $2D$-dimensional space, once for the real part and once for the imaginary part. As a result, there will be an extra factor 2 in Eq. (S10), Eq. (S13), and Eq. (S18). In particular ,

$$\langle \|\vec{y}\|^2 \rangle = -\sigma^2\, \mathrm{Tr}\left(\boldsymbol{A}^{-1}\boldsymbol{G}^{-1}\right) \tag{S31}$$

B. Proof of non-normality of pattern-forming systems

In this section, we prove that for a system described by Eq. (4) of the main text to produce stochastic patterns, it is necessary for $\boldsymbol{J}$ in Eq. (5) of the main text to be non-normal. We show this by finding a lower bound on the difference between the largest eigenvalue of $\boldsymbol{H} = (\boldsymbol{J} + \boldsymbol{J}^T)/2$ and that of matrix $\boldsymbol{J}$. Note that the real part of the largest eigenvalue of a normal matrix is equal to that of its hermitian part. Therefore, this lower bound is a measure of how far from normal the matrix $\boldsymbol{J}$ is.

The proof relies on the fact that for the system to exhibit stochastic patterns, the real part of the largest eigenvalue, λ_1, of $\boldsymbol{K}$ as a function of the length of the wave vector $\vec{k}$ should peak at some value $\vec{k}_0 \neq 0$ [3, 4], and therefore,

$$\delta = \Re(\lambda_1(\boldsymbol{K}_0)) - \Re(\lambda_1(\boldsymbol{J})) > 0, \tag{S32}$$

for $\boldsymbol{K}_0 = \boldsymbol{K}(\vec{k}_0)$. It is a well known fact that the real part of the largest eigenvalue of a matrix is less than or equal to that of its Hermitian part (*e.g.* see Ref. [5]), therefore,

$$\Re(\lambda_1(\boldsymbol{K}_0)) \leq \lambda_1(\boldsymbol{H} - k_0^2 \boldsymbol{D}). \tag{S33}$$

Since both $\boldsymbol{H}$ and $-k_0^2\boldsymbol{D}$ are Hermitian, by Weyl inequality

$$\lambda_1(\boldsymbol{H} - k_0^2 \boldsymbol{D}) \leq \lambda_1(\boldsymbol{H}) + \lambda_1(-k_0^2 \boldsymbol{D}) = \lambda_1(\boldsymbol{H}) - k_0^2 D_{min}. \tag{S34}$$

Adding $k_0^2\, D_{min} - \Re(\lambda_1(\boldsymbol{J}))$ to both sides of this inequality, we arrive at the inequality given in Eq. (7) of the main text:

$$\lambda_1(\boldsymbol{H}) - \Re(\lambda_1(\boldsymbol{J})) \geq \delta + k_0^2 D_{min}. \tag{S35}$$

Moreover, since the non-normality of $\boldsymbol{J}$ should be independent of the diffusion constants, this lower bound can be extended to the supremum of the right hand side of the inequality (S35) over all the matrices $\boldsymbol{D}$ that produce spatial patterns and their corresponding $\vec{k}_0$. In particular, if a system admits deterministic Turing patterns for some set of diffusion constants, *i.e.* $\Re(\lambda_1(\boldsymbol{K}_0)) > 0$, δ would be greater than $-\Re(\lambda_1(\boldsymbol{J}))$, and therefore $\boldsymbol{J}$ would be reactive (this special case was previously proven by Neubert et al. [6]). In this case, if experimentally measured values of diffusion constants do not fall within the Turing pattern regime, the system is still reactive and capable of exhibiting amplified stochastic patterns.

C. Analysis of model by Ridolfi et al.

1. *From the individual-level model to the corresponding SDEs*

In this section we analyze the stochastic extension of a model proposed by Ridolfi et al. in [7]. At the individual level, the model is defined by the following set of reactions

$$\begin{aligned} &2U_i + V_i \xrightarrow{a} 3U_i + V_i, \qquad V_i \xrightarrow{b} 2V_i, \\ &U_i \xrightarrow{e} \varnothing, \qquad 2V_i + 2U_i \xrightarrow{c} V_i + 2U_i, \end{aligned} \tag{S36}$$

where U_i and V_i represent the species U and V in the site i. Migration between sites is accounted by the diffusion reactions

$$U_i \xrightarrow{\delta_u} U_j, \qquad V_i \xrightarrow{\delta_v} V_j, \qquad j \in \langle i \rangle, \tag{S37}$$

where $\langle i \rangle$ is the set of sites neighboring i, $\delta_u = D_U/\Omega^{2/m}$, $\delta_v = D_V/\Omega^{2/m}$, D_U and D_V are the diffusion constants, and Ω is the volume of each site. The state of the system is specified by the concentration vectors $\vec{q}_i \equiv (u_i, v_i) \equiv (U_i, V_i)/\Omega$.

Each reaction in (S36) and (S37) takes the system from a state $\{\vec{q}_i\}$ to $\{\vec{q}_i'\}$ with probability per unit time $T(\{\vec{q}_i'\}|\{\vec{q}_i\})$. These transition rates are given from the law of mass action:

$$\begin{aligned} T\left(\vec{q}_i + \vec{s}_1 | \, \vec{q}_i\right) &= \Omega a u_i^2 v_i, \qquad T\left(\vec{q}_i + \vec{s}_2 | \, \vec{q}_i\right) = \Omega b v_i, \\ T\left(\vec{q}_i - \vec{s}_1 | \, \vec{q}_i\right) &= \Omega e u_i, \qquad T\left(\vec{q}_i - \vec{s}_2 | \, \vec{q}_i\right) = \Omega c u_i^2 v_i^2, \end{aligned} \tag{S38}$$

and for every $j \in \langle i \rangle$

$$\begin{aligned} T\left(\vec{q}_i - \vec{s}_1, \vec{q}_j + \vec{s}_1 | \, \vec{q}_i, \vec{q}_j\right) &= \Omega \delta_u u_i, \\ T\left(\vec{q}_i - \vec{s}_2, \vec{q}_j + \vec{s}_2 | \, \vec{q}_i, \vec{q}_j\right) &= \Omega \delta_v v_i, \end{aligned} \tag{S39}$$

where we have introduced the definitions

$$\vec{s}_1 = \Omega^{-1} \begin{pmatrix} 1 \\ 0 \end{pmatrix}, \qquad \vec{s}_2 = \Omega^{-1} \begin{pmatrix} 0 \\ 1 \end{pmatrix}. \tag{S40}$$

The master equation for the time evolution of the probability density of finding the system in the state $\{\vec{q}_i\}$ at time t, $P(\{\vec{q}_i\}, t)$ can be written as

$$\frac{\mathrm{d}P(\{\vec{q}_i\}, t)}{\mathrm{d}t} = \sum_{\{\vec{q}_{i'}\}} \left(T(\{\vec{q}_i\}|\{\vec{q}_i'\}) - T(\{\vec{q}_i'\}|\{\vec{q}_i\})\right) \tag{S41}$$

Following [3], we can expand the right hand side of Eq. (S41) to second order in Ω^{-1} obtaining a Fokker-Planck equation corresponding the following set of stochastic differential equations

$$\begin{aligned} \frac{\mathrm{d}u_i}{\mathrm{d}t} &= u_i(a u_i v_i - e) + \delta_u \sum_{j \in \langle i \rangle} (u_j - u_i) + \xi_i(t), \\ \frac{\mathrm{d}v_i}{\mathrm{d}t} &= v_i(b - c u_i^2 v_i) + \delta_v \sum_{j \in \langle i \rangle} (v_j - v_i) + \eta_i(t), \end{aligned} \tag{S42}$$

where ξ_i's and η_i's are zero mean Gaussian noise with correlations

$$\begin{aligned} \langle \xi_i(t) \xi_j(t') \rangle &= \frac{\delta(t - t')}{\Omega} \left(\left(u_i(a u_i v_i + e) + \delta_u \sum_{k \in \langle i \rangle} (u_i + u_k) \right) \delta_{i,j} - \delta_u (u_i + u_j) \chi_{\langle i \rangle}(j) \right), \\ \langle \eta_i(t) \eta_j(t') \rangle &= \frac{\delta(t - t')}{\Omega} \left(\left(v_i(b + c u_i^2 v_i) + \delta_v \sum_{k \in \langle i \rangle} (v_i + v_k) \right) \delta_{i,j} - \delta_v (v_i + v_j) \chi_{\langle i \rangle}(j) \right), \end{aligned} \tag{S43}$$

and the characteristic function, $\chi_{\langle i \rangle}$, of $\langle i \rangle$ is defined as

$$\chi_{\langle i \rangle}(j) = \begin{cases} 1 & j \in \langle i \rangle \\ 0 & j \notin \langle i \rangle \end{cases}. \tag{S44}$$

By defining $\vec{f}(\vec{q}) \equiv (f,\ g) \equiv (u(auv - e),\ v(b - cu^2 v))$, $\vec{\xi}_i \equiv (\xi_i,\ \eta_i)$, $\boldsymbol{\delta} \equiv \mathrm{diag}(\delta_u,\ \delta_v)$, and $(\Delta \vec{q})_i \equiv \sum_{j \in \langle i \rangle} (\vec{q}_j - \vec{q}_i)$, we can cast Eq. (S42) in the simple form

$$\frac{\mathrm{d}\vec{q}_i}{\mathrm{d}t} = \vec{f}(\vec{q}_i) + \boldsymbol{\delta} \, (\Delta \vec{q})_i + \vec{\xi}_i(t). \tag{S45}$$

Equation (S45) is the discrete space version of Eq. (5) of the main text and it is more convenient to use, since the analytical results can be more readily compared to the simulations.

The deterministic part of our model has a fixed point $\vec{q}^* \equiv (u^*,\ v^*) = (ba/ce,\ e^2c/a^2b)$, obtained by setting $\vec{f}(\vec{q})$ equal to zero. We can linearize Eq. (S45) around the fixed point $\vec{q}^*$, by defining $\vec{p}_i \equiv \big((u_i - u^*)/\sqrt{2u^*e},\ (v_i - v^*)/\sqrt{2v^*b}\big)$ which are the rescaled deviations of $\vec{q}_i$ from $\vec{q}^*$,

$$\frac{\mathrm{d}\vec{p}_i}{\mathrm{d}t} = \boldsymbol{J}\vec{p}_i + \boldsymbol{\delta}(\Delta\vec{p})_i + \vec{\xi}_i(t), \tag{S46}$$

and where the linear stability operator $\boldsymbol{J}$ is defined as the Jacobian matrix of the transformed function f at the fixed point $\vec{p} = 0$:

$$\boldsymbol{J} = \begin{pmatrix} e & \frac{b^{\frac{3}{2}}a^{\frac{3}{2}}}{ce} \\ -\frac{2e^2c}{a^{\frac{3}{2}}b^{\frac{1}{2}}} & -b \end{pmatrix}. \tag{S47}$$

Evaluating Eq. (S43) at $\vec{q}^*$ yield

$$\begin{aligned} \langle \xi_i(t)\xi_j(t')\rangle &= \frac{\delta(t-t')}{\Omega}\Big(\big(1+\delta_u n/e\big)\delta_{i,j} - \delta_u \chi_{\langle i\rangle}(j)\Big), \\ \langle \eta_i(t)\eta_j(t')\rangle &= \frac{\delta(t-t')}{\Omega}\Big(\big(1+\delta_v n/b\big)\delta_{i,j} - \delta_v \chi_{\langle i\rangle}(j)\Big), \end{aligned} \tag{S48}$$

where $n \equiv |\langle i\rangle|$ is the number of neighbors of each site. Note that for $b > e$, both of the eigenvalues of $\boldsymbol{J}$ have negative real parts, hence $\vec{q}^*$ is an attractor of the dynamics in the absence of the diffusion.

To examine the spatial stability of $\vec{q}^*$, we need to diagonalize the discrete Laplacian operator Δ, by defining the discrete Fourier transform of a sequence $\{s_{\vec{n}}\}$ as

$$\tilde{s}_{\vec{k}} \equiv \big(\mathcal{F}[\{s_{\vec{n}}\}]\big)_{\vec{k}} \equiv \frac{1}{\sqrt{N^D}} \sum_{\vec{n}} \mathrm{e}^{-2\pi \vec{k}.\vec{n}/N} s_{\vec{n}}. \tag{S49}$$

We drop the tildes on the Fourier variable with the convention that the variables with index $\vec{k}$ are Fourier variables. Equation (S46) under this transformation becomes

$$\frac{\mathrm{d}\vec{p}_{\vec{k}}}{\mathrm{d}t} = \boldsymbol{K}\vec{p}_{\vec{k}} + \vec{\xi}_{\vec{k}}(t), \qquad \boldsymbol{K} = \boldsymbol{J} + \Delta(\vec{k})\boldsymbol{\delta}, \tag{S50}$$

where $\Delta(\vec{k})$ is the discrete Fourier transform of the discrete Laplacian operator given by

$$\Delta(\vec{k}) \equiv -2\sum_{l=1}^{D}\big(1 - \cos(2\pi k_l/N)\big) \tag{S51}$$

and

$$\begin{aligned} \langle \xi_{\vec{k}}(t)\xi^*_{\vec{k}'}(t')\rangle &= \Omega^{-1}\left(1 - e^{-1}\delta_u\Delta(\vec{k})\right)\delta_{\vec{k},\vec{k}'}\delta(t-t'), \\ \langle \eta_{\vec{k}}(t)\eta^*_{\vec{k}'}(t')\rangle &= \Omega^{-1}\left(1 - b^{-1}\delta_v\Delta(\vec{k})\right)\delta_{\vec{k},\vec{k}'}\delta(t-t'). \end{aligned} \tag{S52}$$

In the stochastic patterns regime, the contribution of the diffusion process in the amplitude of the noise in Eq. (S53) is small and can be neglected. This approximation is not necessary, since there is always a change of variables that simplifies the correlation matrix to a multiple of the identity matrix (this is the reason for the rescaling in the definition of $\vec{p}$) but it simplifies the formula. With this approximation we obtain:

$$\left\langle \vec{\xi}_{\vec{k}}(t)\vec{\xi}^{\dagger}_{\vec{k}'}(t')\right\rangle = \Omega^{-1}\delta_{\vec{k},\vec{k}'}\delta(t-t')\,\mathbb{1}_2, \tag{S53}$$

where $\vec{\xi}^{\dagger}_{\vec{k}'}$ is the conjugate transpose of $\vec{\xi}_{\vec{k}'}$, and $\mathbb{1}_2$ is the 2×2 identity matrix.

2. Phase diagram of pattern formation

The pattern forming behavior of the model defined by (S36) can be understood by analyzing the eigenvalues of $\boldsymbol{K}$ as a function of $\vec{k}$. The region of stochastic patterns is defined as the parameter regime in which the largest eigenvalue of $\boldsymbol{K}$ has a peak at some $\vec{k}_0 \neq 0$ with a value larger than its value at $\vec{k} = 0$. The expression of matrix $\boldsymbol{K}$ is obtained using Eq. (S50) and Eq. (S47):

$$\boldsymbol{K} = \begin{pmatrix} e + \Delta(\vec{k})\delta_u & \frac{b^{\frac{3}{2}} a^{\frac{3}{2}}}{ce} \\ -\frac{2e^2 c}{a^{\frac{3}{2}} b^{\frac{1}{2}}} & -b + \Delta(\vec{k})\delta_v \end{pmatrix} \tag{S54}$$

Most of the properties of the system depend on the following three parameters,

$$\rho = \frac{b}{e}, \qquad \nu = \frac{e\,c}{a^{\frac{3}{2}} b^{\frac{1}{2}}}, \qquad r = \frac{\delta_v}{\delta_u} = \frac{D_V}{D_U}, \tag{S55}$$

which we can use to write matrix $\boldsymbol{K}$ as

$$\boldsymbol{K} = \begin{pmatrix} e + \Delta(\vec{k})\delta_u & b/\nu \\ -2e\,\nu & -b + \Delta(\vec{k})\delta_v \end{pmatrix}. \tag{S56}$$

The largest eigenvalue of $\boldsymbol{K}$ is given by

$$\lambda(\vec{k}) = \frac{1}{2}\left(\sqrt{b^2 - 2b\Delta(\vec{k})(\delta_v - \delta_u) - 6be + \Big(e - \Delta(\vec{k})(\delta_v - \delta_u)\Big)^2} - b + \Delta(\vec{k})(\delta_v + \delta_u) - e\right). \tag{S57}$$

We notice that the eigenvalues of $\boldsymbol{K}$ are independent of ν. For small $\vec{k}$, $\Delta(\vec{k})$ is a monotonically decreasing function of $\vec{k}$ (proportional to $-k^2$). We introduce the notation $y \equiv -\Delta(\vec{k})$. To determine if λ monotonically decays or if it has a maximum at some $\vec{k}_0 \neq 0$, we can differentiate λ with respect to y and see if it has a positive root. The largest root of $\frac{\mathrm{d}\lambda}{\mathrm{d}y}$ is given by

$$y_0 = -\Delta(\vec{k}_0) = \frac{(r+1)\sqrt{2\,b\,e\,r} - b\,r - e\,r}{\delta_u\,(r-1)\,r}. \tag{S58}$$

For y_0 to be greater than zero we need

$$\rho < \frac{\left(1 + r + r^2 + (r+1)\sqrt{r^2+1}\right)}{r}. \tag{S59}$$

We can find the condition on the ratio of the diffusion constants by inverting this inequality:

$$r > \frac{1 - 2\,\rho + \rho^2 + (1+\rho)\sqrt{1 + \rho\,(\rho - 6)}}{4\,\rho} = f_1(\rho). \tag{S60}$$

The condition for formation of stochastic pattern is $\lambda(\vec{k}_0) > \Re(\lambda(0))$. We can find $\lambda(\vec{k}_0)$ and $\lambda(0)$ by substituting $y_0 = y(\vec{k}_0)$ from Eq. (S58) and $y(0) = 0$ in Eq. (S57):

$$\lambda(\vec{k}_0) = \frac{b + e\,r - \sqrt{8\,b\,e\,r}}{r-1}, \qquad \lambda(0) = \frac{1}{2}\left(\sqrt{b^2 - 6\,b\,e + e^2} - b + e\right). \tag{S61}$$

Then, $\lambda(\vec{k}_0) > \Re(\lambda(0))$ simplifies to

$$r > \frac{-1 + 14\,\rho - \rho^2 + 4\sqrt{-2\,\rho\,(1 + \rho\,(\rho - 6))}}{(1+\rho)^2} = f_2(\rho). \tag{S62}$$

Condition for deterministic Turing pattern is a lot simpler; we just need $\lambda(\vec{k}_0) > 0$ which simplifies to

$$r > \left(3 + 2\sqrt{2}\right)\rho = f_3(\rho). \tag{S63}$$

When r is greater than $f_1(\rho)$ and $f_2(\rho)$ but less than $f_3(\rho)$, the system exhibits stochastic patterns (blue region in Fig. 4 of the main text), while we observe the deterministic patterns when r is greater than f_3 (orange region of Fig. 4 of the main text).

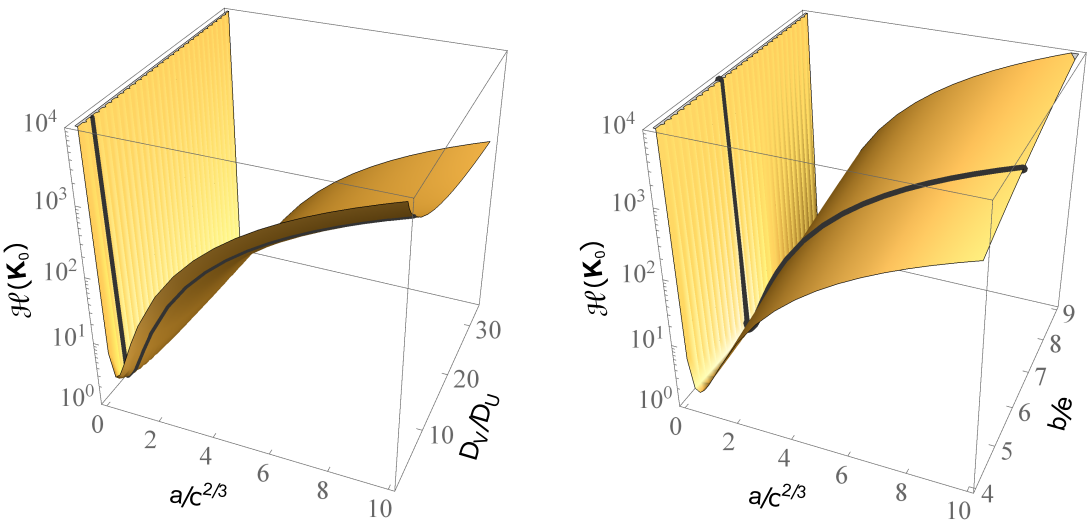

FIG. S1. Nonnomrality index as a function of $r = D_V/D_U$, $\rho = b/e$, and $a/c^{2/3}$. (Left) Constant $\rho = 5.8$. (Right) Constant $r = 3.4$. The thick black curve corresponds to the point P on Fig. 4 of the main text.

3. Non-normality index of the model

The amplification of the stochastic patterns depend on the non-normality index of $\boldsymbol{K}_0 = \boldsymbol{K}(\vec{k}_0)$ given by

$$\boldsymbol{K}_0 = \begin{pmatrix} e - y_0\,\delta_u & b/\nu \\ -2\,e\,\nu & -b - y_0\,\delta_v \end{pmatrix}, \tag{S64}$$

where $y_0 \equiv -\Delta(\vec{k}_0)$. We use Eq. (S21) to calculate the non-normality index of $\boldsymbol{K}_0$:

$$\mathcal{H}(\boldsymbol{K}_0) = 1 + \left(\frac{b + 2e\nu^2}{\nu(b - e + y_0\,(\delta_u + \delta_v))} \right)^2. \tag{S65}$$

We substitute y_0 from Eq. (S58) and rewrite the resulting expression in terms of ρ, r, and ν, arriving at

$$\mathcal{H}(\boldsymbol{K}_0) = 1 + \left(\frac{2\nu^2 + \rho}{\nu\left(\rho - 1 + \frac{(r+1)\left(-\rho r + (r+1)\sqrt{2\rho\, r} - r\right)}{(r-1)r}\right)} \right)^2. \tag{S66}$$

Since the eigenvalues of $\boldsymbol{K}$ do not depend on ν, one can change $\mathcal{H}(\boldsymbol{K}_0)$ by changing ν without moving the system in its phase diagram (see Fig. 4 of the main text). This can be done by changing the ratio of $a/c^{2/3}$ without affecting ρ. Figure S1 is the extension of the right panel of Fig. 4 of the main text for different values of r at constant ρ and different values of ρ at constant r (provided per request of the referee), showing that the particular choice of the point P does not affect the shape of this graph, and the parameters are not fine-tuned to achieve high nonnormality index.

[1] C. W. Gardiner, *Handbook of Stochastic Methods for Physics, Chemistry and the Natural Sciences*, 4th ed. (Springer, New York, 2009).
[2] N. G. van Kampen, *Stochastic Processes in Physics and Chemistry*, 3rd ed. (Elsevier Science, Amsterdam, 2007).
[3] A. J. McKane, T. Biancalani, and T. Rogers, Bull. Math. Biol. **76**, 895 (2014).
[4] T. Biancalani, D. Fanelli, and F. Di Patti, Phys. Rev. E **81**, 046215 (2010).
[5] M. Adam and M. J. Tsatsomeros, Electron. J. Linear Algebra **15**, 239 (2006).
[6] M. G. Neubert, H. Caswell, and J. Murray, Mathematical biosciences **175**, 1 (2002).
[7] L. Ridolfi, C. Camporeale, P. D'Odorico, and F. Laio, Eur. Phys. Lett. **95**, 18003 (2011).